

See discussions, stats, and author profiles for this publication at: <https://www.researchgate.net/publication/221759009>

A DNA-Based Nanomechanical Device Used To Characterize the Distortion of DNA by Apo-SoxR Protein

ARTICLE in BIOCHEMISTRY · FEBRUARY 2012

Impact Factor: 3.02 · DOI: 10.1021/bi201196s · Source: PubMed

CITATIONS

6

READS

56

4 AUTHORS, INCLUDING:



Bruce Demple

Stony Brook University

192 PUBLICATIONS 15,196 CITATIONS

[SEE PROFILE](#)



Nadrian C. Seeman

New York University

315 PUBLICATIONS 23,246 CITATIONS

[SEE PROFILE](#)

A DNA-Based Nanomechanical Device Used To Characterize the Distortion of DNA by Apo-SoxR Protein

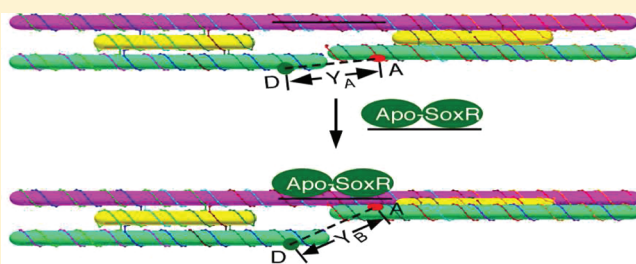
Chunhua Liu,[†] Eunsuk Kim,^{‡,§} Bruce Demple,[‡] and Nadrian C. Seeman*,[†]

[†]Department of Chemistry, New York University, 100 Washington Square East, New York, New York 10003, United States

[‡]Department of Pharmacological Sciences, Stony Brook University School of Medicine, BST 8, Room 140, Stony Brook, New York 11790, United States

Supporting Information

ABSTRACT: DNA-based nanomechanical devices can be used to characterize the action of DNA-distorting proteins. Here, we have constructed a device wherein two DNA triple-crossover (TX) molecules are connected by a shaft, similar to a previous device that measured the binding free energy of integration host factor. In our case, the binding site on the shaft contains the sequence recognized by SoxR protein, the apo form of which is a transcriptional activator. Another active form is oxidized [2Fe-2S] SoxR formed during redox sensing, and previous data suggest that activated Fe-SoxR distorts its binding site by localized DNA untwisting by an amount that corresponds to ~2 bp. A pair of dyes report the fluorescence resonance energy transfer (FRET) signal between the two TX domains, reflecting changes in the shape of the device upon binding of the protein. The TX domains are used to amplify the signal expected from a relatively small distortion of the DNA binding site. From FRET analysis of apo-SoxR binding, the effect of apo-SoxR on the original TX device is similar to the effect of shortening the TX device by 2 bp. We estimate that the binding free energy of apo-SoxR on the DNA target site is 3.2–6.1 kcal/mol.



Nanomechanical devices have been developed widely during the past decade.¹ Among such devices, those based on DNA have become significant tools in recent years for fine measurements of nanoscale objects, because of their predictability, rigidity, and precise structural control (e.g., refs 2–7). The first robust DNA-based nanomechanical device³ was based on the B–Z transition,⁸ wherein a DNA domain is switched from one side of a DNA double helix to the other when the proto-Z region of the device is converted from the B-DNA conformation to the Z-DNA conformation in the presence of $\text{Co}(\text{NH}_3)_6^{3+}$; this transition was demonstrated by fluorescence resonance energy transfer (FRET) measurements.³

Our laboratory has reported a protein-driven DNA nanomechanical device based on the triple-crossover (TX) motif⁹ that has been used to measure the excess binding energy of *Escherichia coli* integration host factor (IHF).⁶ In this case, IHF, a small sequence-specific DNA binding protein, induces a sharp bend (more than 160°) in the DNA helix¹⁰ of the TX device, of which the operation is monitored by FRET. Here, we are examining a different protein, SoxR, to investigate whether it can induce a distortion in the DNA duplex. Previous data¹¹ suggest that this is the case, which we tested using the DNA nanomechanical device.

SoxR in *E. coli* is a redox-sensing transcription activator that responds to signals generated by superoxide-generating agents or nitric oxide,¹² as well as to metal chelators (H. Ding,

E. Hidalgo, and B. Demple, Transcriptional activity of apo-SoxR protein dependent on negative supercoiling of the DNA, manuscript submitted for publication). SoxR is a member of a protein family typified by MerR, which reacts with Hg^{2+} to trigger transcription via localized distortion of DNA structure. Such distortions are necessary because the target promoters for MerR and related proteins are “overwound” by having key recognition elements for RNA polymerase separated by 2 bp more than the optimal 17 bp. Topological assays of MerR were consistent with a possible untwisting mode for its action, although the presence of multiple MerR binding sites in the DNA molecules studied¹³ left open the possibility that some topological effects were due to the interaction of bound MerR proteins with each other. Previous studies suggested that this ability to restructure DNA is shared by SoxR in acting on the promoter of the *soxS* gene.¹¹ Footprinting studies indicate such SoxR-mediated distortions in *soxS* promoter DNA, and 1–2 bp shortening of the distance separating the RNA polymerase elements strongly activates SoxR-independent transcription. A [2Fe-2S] center in each subunit of SoxR is required for redox activation or the response to NO. This requirement relates not to the protein’s affinity for DNA but rather to SoxR’s ability to restructure the *soxS* promoter. Unfortunately, strong FRET

Received: August 3, 2011

Revised: January 11, 2012

Published: January 17, 2012

fluorophore quenching by the iron–sulfur centers has restricted analysis to apo-SoxR. Although it is not redox-sensitive, apo-SoxR exhibits ~10% of the transcription activating capacity found for oxidized Fe-SoxR.¹⁴ The details of the chemical differences among the three different activated forms of SoxR are indicated in Figure 1. Measuring the distortion of DNA by

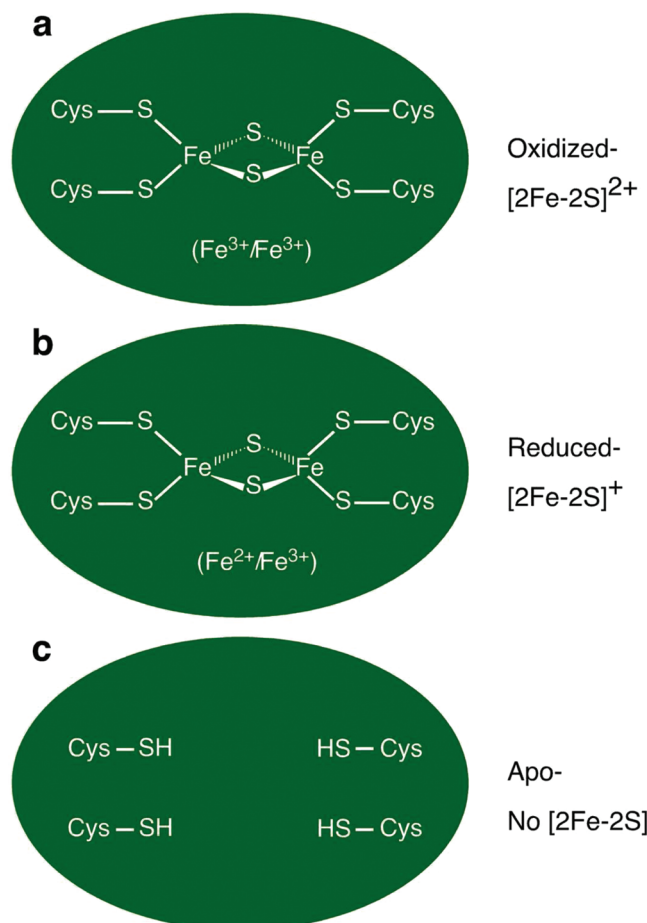


Figure 1. Structures of [2Fe-2S] clusters in distinct states of SoxR. (a) Oxidized form. SoxR with oxidized [2Fe-2S]²⁺ centers is a potent activated form of the transcription factor.^{11,12} (b) Reduced form. SoxR with reduced [2Fe-2S]⁺ centers is an inactive form of the transcription factor.^{11,12} (c) Apo form. SoxR without [2Fe-2S] centers is another activated form of the transcription factor.^{14,32}

SoxR with a well-built DNA-based nanomechanical device not only provides us with a specific case of the application of a DNA nanomechanical device in molecular biology but also offers us vital clues for the structural and functional analysis of SoxR protein. The solution approach taken here is complementary to the recent crystallographic structural investigation of Fe-SoxR.¹⁵

The DNA double-crossover (DX) nanomechanical device reported previously could detect a 180° rotation due to the B–Z DNA transition based on the change in the distance detected by FRET.³ However, this device is not sufficiently large for the study of a much smaller distortion. We therefore designed a new DNA nanomechanical device that can overcome the disadvantages of a DX-based device, as well as a low-yield problem noted for the initial design of a topologically closed TX-based device;¹⁶ this new device can avail itself of the advantages of the IHF-driven device while using apo-SoxR to drive it.

The DNA triple-crossover nanomechanical device constructed here contains the basic elements of the IHF-driven DNA nanodevice⁶ and is more complex and sensitive than the B–Z DNA transition DX device.³ Figure 2 shows that it is composed of two TX motifs connected by 58 nucleotide pairs in the top domain (junction to junction) containing the specific SoxR binding site in the middle of the top domain; this is more than enough space to accommodate the protein, which is ~70 Å long. As with the IHF device, a cohesive tract connecting the bottom domains has been installed to keep the system in a well-defined initial conformation. In contrast to the IHF device, where the purpose of the tract is to provide an energy barrier for the protein, the point of the cohesive tract here is to select a specific starting conformation from the ensemble that would be present in its absence. The connecting helix is insufficiently rigid to provide a single conformation in this system, although with SoxR bound, we are able to obtain a meaningful FRET reading. Despite the tract, it is capable of being distorted by the binding of apo-SoxR to its site. The increased spatial sensitivity derived from using the TX device allows us to detect the smaller rotational distortions of the DNA duplex, predicted for the binding of SoxR. The operation of the DNA nanodevice is demonstrated by an electrophoretic mobility shift assay (EMSA) and FRET experiments.

MATERIALS AND METHODS

Design, Synthesis, and Purification of DNA. The apo-SoxR binding complex, an open-version TX nanomechanical device, was designed as shown in Figure 2. The sequences of

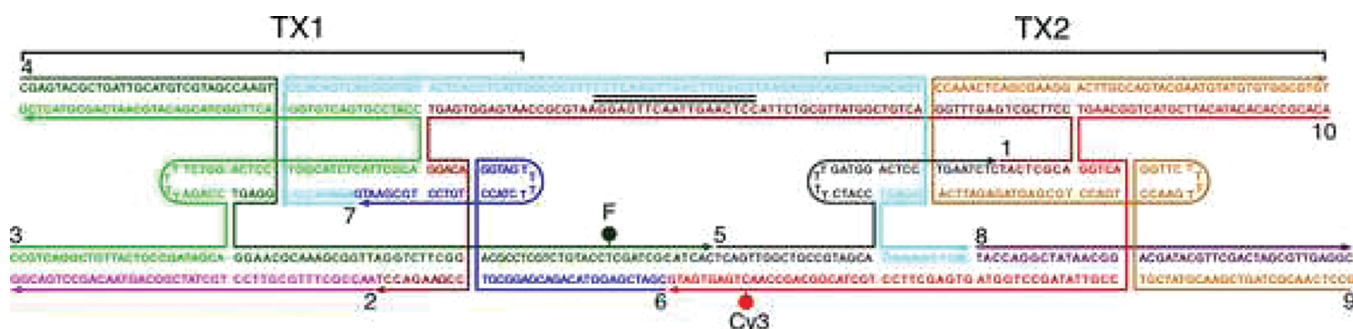


Figure 2. Structure and sequence of the TX device. The device consists of 10 DNA single strands labeled in Arabic numerals and depicted in different colors. The individual TX motifs are labeled TX1 and TX2. The 3' ends of the strands are shown by arrowheads. The 24 bp *soxS* promoter sequence with the 18 bp SoxR binding site underlined is in the middle of the top domain within strands 1 and 7. The bottom domains are connected by a cohesive tract. The length of the cohesive tract can be changed as desired. Crossovers between strands are shown as connections. Fluorescein and Cy3 are represented by a green F and a red Cy3, respectively, on the bottom domains.

the strands in Figure 3 were designed with SEQUIN¹⁷ by applying the principles of sequence symmetry minimization.¹⁸

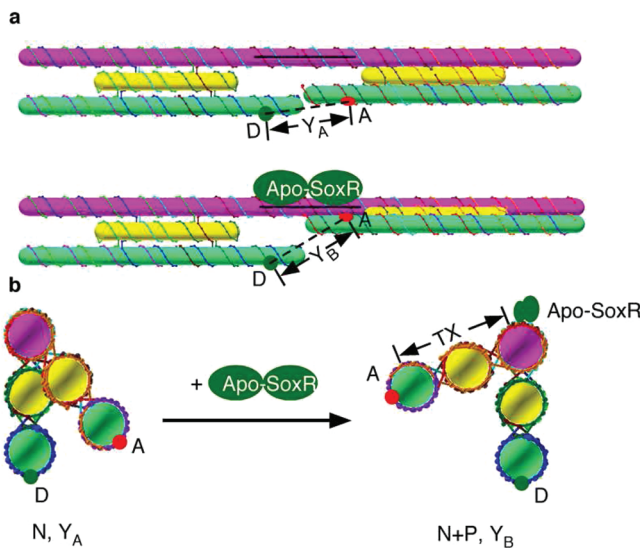


Figure 3. Scheme and action of the TX device. (a) Molecular model of the operation of the TX device from the front view. This device contains two TX DNA molecules connected by 58 nucleotide pairs (junction to junction) of duplex DNA along the top domain. The top, middle, and bottom domains of the device are shown as pink, yellow, and green cylinders, respectively. The apo-SoxR specific binding sequence is highlighted by a black line in the center of the top DNA duplex. Apo-SoxR, a homodimer, is drawn as two adjacent green solid ellipses. Two circles are attached to the bottom domains of the device. The green circle represents fluorescein as a donor, and the red one represents Cy3 as an acceptor. The top and bottom panels show the original device without and with apo-SoxR, respectively. The corresponding distances between the two dyes are marked by Y_A (unbound, N) and Y_B (bound, N+P). (b) Right-hand side view of the TX device in panel a. The unbound and bound devices are denoted as N and N+P, respectively. With the binding of apo-SoxR protein, the device is distorted, and the distance between the two dyes increases from Y_A to Y_B . The cartoons shown here are highly simplified forms showing the difference in distance with and without the protein. A detailed protein structure for apo-SoxR is not available.

The individual DNA strands used in this study were purchased from Integrated DNA Technology (Coralville, IA) or were synthesized on an Applied Biosystems 394 automatic DNA synthesizer, removed from the support, and deprotected using routine phosphoramidite procedures.¹⁹ All the DNA strands were purified by denaturing polyacrylamide gel electrophoresis at 55 °C. Bands of the target size were cut from 8 to 20% denaturing gels and eluted in a solution containing 500 mM ammonium acetate, 10 mM magnesium acetate, and 1 mM EDTA overnight at 4 °C. The eluates were extracted with *n*-butanol to remove ethidium bromide, followed by ethanol precipitation for recovery.

Fluorescein-labeled strand 5 was the product of incorporating fluorescein-dT phosphoramidite (Glen Research) in the oligonucleotide synthesis. Cy3 labeling was done by filling-in Cyanine 3-dCTP (Perkin-Elmer), using Klenow fragment polymerase (NEB), following a protocol suggested by the supplier. First, 1000 pmol of DNA template and primer was annealed in 200 μL of 1× Eco Pol buffer (polymerase reaction buffer) via a fast annealing protocol: 5 min at 90 °C, 30 min at 65 °C, 30 min at 45 °C, and 30 min at 37 °C. At this point, 100 nmol of the specified free dNTPs, 300 nmol of dCTP-Cy3,

and 2 units of Klenow fragment polymerase (NEB) were added to the sample, and the mixture was incubated at 37 °C for ~1.5 h, followed by ethanol precipitation and gel purification.

Denaturing Polyacrylamide Gel Electrophoresis. Gels contained 8–20% acrylamide (80:1 acrylamide:bisacrylamide ratio) and 8.3 M urea. The running buffer consisted of 89 mM Tris-HCl (pH 8.0), 89 mM boric acid, and 2 mM EDTA (TBE). The sample buffer consisted of 10 mM NaOH, 1 mM EDTA, 0.1% bromophenol blue, and 0.1% xylene cyanol FF tracking dye. Gels were run on a Hoefer SE 600 electrophoresis unit at 55 °C (31 V/cm, constant voltage).

Phosphorylation. DNA strands (600 pmol) were dissolved in 40 μL of a solution containing 66 mM Tris-HCl (pH 7.6), 6.6 mM MgCl₂, and 10 mM dithiothreitol (DTT) and mixed with 2 μL of 2.2 μM [γ -³²P]ATP (10 μCi/μL) and 2 units of polynucleotide kinase (U.S. Biochemical) for 90 min at 37 °C. The reaction was stopped when the solution was heated to 90 °C for 10 min, followed by phenol/chloroform extraction, ethanol precipitation, and gel purification.

Ligation. Two units of T4 polynucleotide ligase (Amersham) was added to the annealed samples in a 1× ligation buffer supplied by the manufacturer, and the mixtures were incubated at 16 °C overnight. The reaction was then stopped when the solution was heated to 90 °C for 10 min, followed by phenol/chloroform extraction, ethanol precipitation, and gel purification.

Formation of Hydrogen-Bonded DNA Nanomechanical Devices. DNA nanomechanical devices were formed by mixing a stoichiometric quantity of each strand (100 nM), as estimated by OD₂₆₀, in apo-SoxR protein binding buffer [75 mM KCl, 10 mM Tris-HCl (pH 7.5), 0.25 mM EDTA, 2.0 mM DTT, 10% glycerol, and 1.5 mM Mg²⁺]. These mixtures were preheated to 90 °C and cooled slowly over 48 h to room temperature in a 2 L water bath. The stoichiometry was determined by titrating pairs of strands designed to hydrogen bond together and visualizing them by nondenaturing gel electrophoresis; the absence of monomer bands could be taken to indicate the end point.²⁰

Formation of Apo-SoxR–DNA Complexes. A 35 μM apo-SoxR stock solution²¹ was added to aliquots of 100 μL of 100 nM DNA nanomechanical device up to a final apo-SoxR concentration of 500 nM, and the mixture was incubated at room temperature for 15 min before each measurement.

Electrophoretic Mobility Shift Assay. Apo-SoxR–DNA complexes (25 μL) were loaded on a 0.7% agarose gel with 2.5 μL of a solution containing 50% glycerol, 0.02% bromophenol blue, and 0.02% xylene cyanol FF tracking dyes. Gels were run in the buffer containing 20 mM Tris-HCl (pH 8.0), 3.0 mM sodium acetate (pH 7.9), and 1.0 mM EDTA at 100 V for 2.5 h at 4 °C.

Spectroscopic Methods. OD₂₆₀ was measured on a SPECTRONIC GENESYS 5 spectrophotometer. The steady-state fluorescence intensity of the devices was measured using an AMINCO BOWMAN Series 2 spectrometer at room temperature. The emission spectra were corrected for instrument response, lamp fluctuations, and buffer contributions. The theoretical values of FRET were calculated according to the methods described in previous studies.^{3,6,22,23}

Molecular Models. All the molecular models in this article were generated by GIDEON, a program for designing and analyzing complex DNA structure.²⁴

RESULTS AND DISCUSSION

A structural schematic and the operation of the DNA TX device are shown in Figure 3. Panel a displays the action of the TX device from the front. The top panel illustrates the DNA device without apo-SoxR. Two rigid TX motifs are connected by a 58 bp DNA duplex (junction to junction in the top domain) with a 24 bp *soxS* promoter sequence region, with the 18 bp SoxR binding site in the middle. The ends of the top and bottom domains are open so they can release strand stress without affecting the rigidity of the device, while the ends of the middle domains are closed with dT₄ hairpin loops to ensure the stability of the motifs. The bottom domains are connected by a short cohesive tract to keep the initial state of the system as close to planar as possible. Two dyes, fluorescein as a donor and Cy3 as an acceptor, are attached to the bottom domains, indicated by green and red circles, respectively. The distance between these two dyes is short enough for FRET to occur and to be measured. The bottom panel indicates the DNA device with apo-SoxR. The protein binds to its recognition site on DNA, and the figure shows the distance between two dyes is changed. The change in distance is magnified by the TX lever arms, thus varying the FRET signal, which is proportional to the inverse sixth power of the distance between two dyes.^{25,26} This DNA nanodevice contains a structure similar to the IHF-driven device but is designed to detect the rotation of the DNA double helix induced by apo-SoxR. The experimental measurement is ultimately a change in distance between two points, which may, of course, reflect elements of both bending and unwinding.

Panel b of Figure 3 shows a right side view of the TX device on panel a. For comparison, the distances between two fluorescent dyes before and after distortion in the TX device are indicated as Y_A and Y_B, respectively. With the binding of apo-SoxR protein, the distance between two dyes in the TX device increases and the magnitude of the FRET signal decreases. Consequently, this system combines the strengths of the IHF-driven device⁶ and the B-Z device³ and is designed to be useful in fulfilling our attempt to monitor a relatively small distortion.

The donor energy transfer efficiency of a series of DNA devices differing in the lengths of their cohesive tracts is illustrated in Figure 4. The sequence of the DNA cohesive tract is 5'-CGCATCAC/TC-3':3'-GC/GTAGTGAG-5' (the slashes

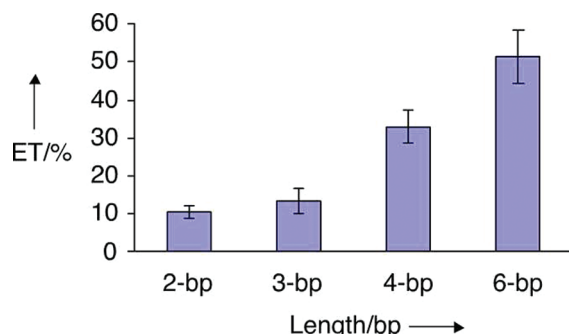


Figure 4. FRET measurements of the device as a function of the length of the device cohesive tract. The donor energy transfer efficiencies of the devices are shown as blue columns. The ranging of the base pairs within the cohesive tract is changed from two to six. The corresponding energy transfer measurements are labeled as 2-bp, 3-bp, 4-bp, and 6-bp. Each measurement was performed three times. Standard deviations are indicated by the error bars.

indicate nicks), the same as that used in ref 6. We use different nicking positions to produce sticky ends within the cohesive tract that contain two, three, four, and six nucleotide pairs. From the small energy transfer of the devices in the absence of protein, we conclude that sticky ends containing two or three nucleotide pairs are insufficient to hold the system stable. Sticky ends containing four and six nucleotide pairs are appropriate. We have conducted all the following experiments by adopting the former because it is the appropriate system containing the fewest sticky ends.

The formation, appropriate binding condition, and ratio of apo-SoxR to the DNA device have been determined by an EMSA through the titration (shown as Figure S1 of the Supporting Information). Complete binding of the TX device by apo-SoxR occurred when the molar ratio of protein to DNA was $\geq 5:1$.

The binding of the DNA nanomechanical devices by apo-SoxR used in the FRET measurements is illustrated in Figure 5.

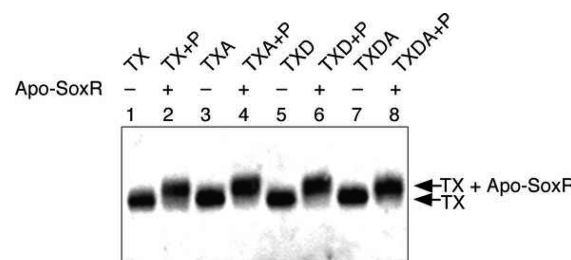


Figure 5. Electrophoretic mobility shift assay of apo-SoxR bound to the TX devices. Apo-SoxR was added to the TX devices in the apo-SoxR binding buffer with a 5:1 protein:DNA molar ratio. Lanes 1, 3, 5, and 7 contained TX devices without dyes (TX), with Cy3 (acceptor, TXA), with fluorescein (donor, TXD), and with both fluorescein and Cy3 (donor and acceptor, TXDA), respectively. Lanes 2, 4, 6, and 8 contained the mixture of apo-SoxR with the TX devices in lanes 1, 3, 5, and 7, respectively.

Odd-numbered lanes contained the four individual devices without dyes (lane 1, TX), with acceptor Cy3 (lane 3, TXA), with donor fluorescein (lane 5, TXD), and with both donor fluorescein and acceptor Cy3 (lane 7, TXDA). Addition of apo-SoxR to the devices is shown in lane 2 (TX+P), lane 4 (TXA+P), lane 6 (TXD+P), and lane 8 (TXDA+P). The molar ratio of DNA to protein was 1:5. The lower mobilities of the protein-bound DNA species in the respective lanes demonstrate clearly the binding of the DNA nanodevice by apo-SoxR. The single bands seen for the bound DNA lanes indicate complete binding of the DNA with apo-SoxR.

Figure 6a shows the comparison of the FRET signal of the device bound by apo-SoxR with those of the original TX device (N0), the devices with a single-base pair deletion (N-1), and a double-base pair deletion (N-2) from the original TX device. The three parts of the top panel, from left to right, display the N0, N-1, and N-2 devices, respectively. The value we measure for apo-SoxR distorting the TX device (N+P), as seen in the bottom panel, is between those of the N-1 and N-2 devices, and relatively close to that of the N-2 device.

To confirm that the variation in the FRET signal observed from the unbound and bound DNA nanodevice is caused by distortion due to apo-SoxR, we designed another control system, similar to the original, except that the specific apo-SoxR binding site was replaced with a nonspecific one (Figure 6b). The FRET signals before (Non-S) and after (Non-S+P) the

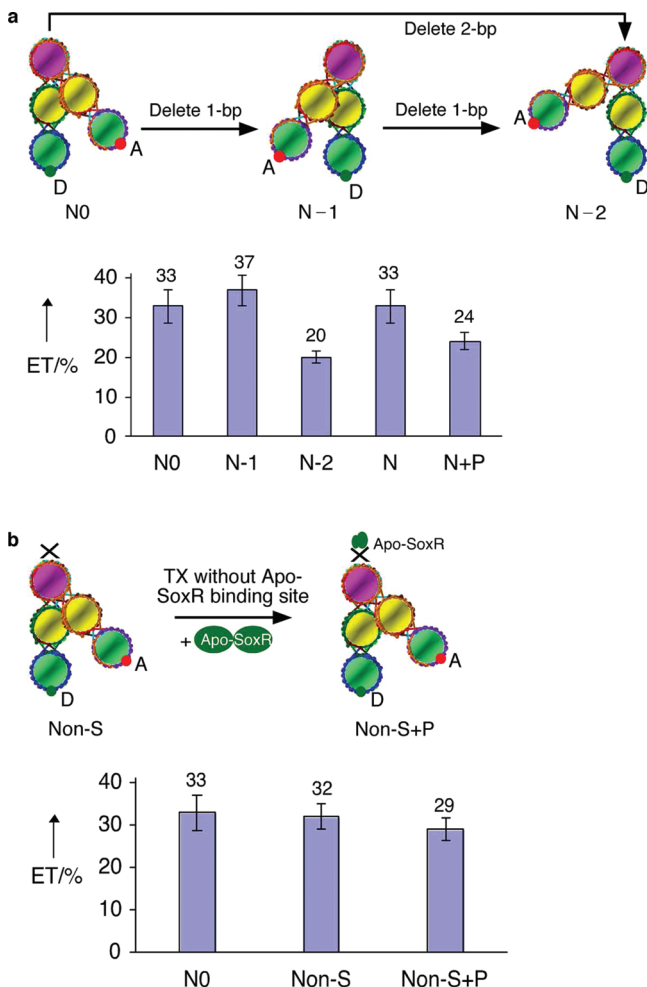


Figure 6. Determination of device operation using FRET. (a) Comparing the FRET signal of the device bound by apo-SoxR with those of three control systems. Each measurement was performed three times. Standard deviations are indicated by the error bars. Schematics of the control systems, including the original TX device (N0), the devices with a single-base pair deletion (N-1), and devices with a double-base pair deletion (N-2), are shown in the top panel. Their corresponding energy transfer values are 33, 37, and 20%, respectively, as shown in the blue columns in the bottom panel. When apo-SoxR is bound to the TX device (N+P), the magnitude of the energy transfer signal is decreased to 24%. The bending rigidity (or persistence length, a , in nanometers) and DNA helical repeat (γ , in base pairs per turn) can be determined using dinucleotide models.³⁵ The corresponding persistence lengths for these devices are 49.3, 49.3, and 49.6 nm, respectively; the corresponding DNA helical repeats in this case are 10.48, 10.49, and 10.48 bp/turn, respectively. The calculation is based on the parameters provided by ref 35. (b) Behavior of the control system lacking the apo-SoxR binding site. The states of this control device for both unbound (Non-S) and bound (Non-S+P) molecules are illustrated in the top panel. In the bottom panel, the FRET signals from the experiments in the absence (Non-S) and presence (Non-S+P) of apo-SoxR are shown and compared with that of the original TX device (N0).

addition of apo-SoxR, shown as the columns in Figure 6b, are approximately identical, and close to that of the original TX device, N0. This observation suggests that apo-SoxR is incapable of distorting the control device without the protein's specific binding site. This experiment rules out the side effects of the protein, such as quenching, dilution, or nonspecific binding, on the FRET signals and further proves the distortion is due to apo-SoxR acting on the device.

Recently, the crystal structure of the [2Fe-2S] SoxR–soxS promoter complex was reported, revealing a bound 20 bp DNA duplex with the 18 bp soxS binding site bent 65° by the [2Fe-2S] SoxR in the center of the binding site toward the major groove.¹⁵ The bound duplex is distorted by a combination of bending and rotation.¹⁵ Were this distortion confined strictly to rotation, it would correspond to ~3 bp worth of rotation, ~102°. This result provides another possible explanation of the distance shortening of the soxS promoter with apo-SoxR, in addition to simple rotation.¹¹ The distortion estimate we find from FRET is a smaller distortion (interpreted completely as rotation, to put them on the same scale) corresponding to ~68° (2 bp). This deviation might be caused by several factors: (a) the different experimental environments in solution versus the crystal, (b) the different distortion modes for apo-SoxR and Fe-SoxR, and (c) the interference by the sticky-ended cohesion.

Figure 7 displays the donor energy transfer efficiency monitored by the operation of the DNA devices with various

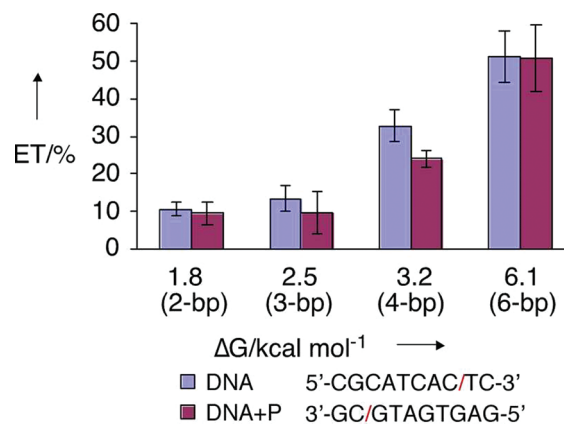


Figure 7. Donor energy transfer of devices upon apo-SoxR binding. The donor energy transfer efficiencies measured without (DNA, in blue) and with (DNA+P, in red) apo-SoxR are shown as the pairs of colored columns. Each measurement was performed three times. Standard deviations are indicated by the error bars. The length of the base pairs within the cohesive tract is varied from two to six. The abscissa shows the estimated molar free energy available, based on the nearest-neighbor approximation. Nearest-neighbor corrections for Mg²⁺ follow from refs 33 and 34. The end point of the binding free energy for apo-SoxR is between 3.2 and 6.1 kcal/mol.

sticky end lengths upon apo-SoxR binding. The pairs of colored columns show the comparison of energy transfer (ET) before (DNA, blue) and after (DNA+P, red) the binding of apo-SoxR. Each measurement was performed three times. The sequence of the DNA cohesive tract is the same as that used in Figure 4. We changed the length of the overlap region systematically over a range of two to six nucleotide pairs. The corresponding standard free energy of the overlap region is shown as the abscissa. The changes in the standard free energy, enthalpy, and entropy are summarized in Table 1. The parameters are from refs 27 and 28, with others for the nicks and dangling ends, generously supplied by J. SantaLucia. We ascribe the relatively small amount of transfer before addition in the low-energy measurement to fraying of the small cohesive ends present. The energy transfer observed following addition of apo-SoxR increases as we increase the number of base pairs along the cohesive tract. The FRET difference with and without protein suggests that the system with sticky ends containing four nucleotide pairs [3.2 kcal/mol (Table 1)] is tethered in place

Table 1. Nearest-Neighbor Thermodynamic Parameters for DNA Base Pair Dissociation

Propagation Sequence ^a	$\bullet H^\circ$ (kcal mol ⁻¹)	$\bullet S^\circ$ ^b (kcal mol ⁻¹ K ⁻¹)	$\bullet S^\circ$ ^c (kcal mol ⁻¹ K ⁻¹)	$\bullet G^\circ$ ^b (kcal mol ⁻¹)	$\bullet G^\circ$ ^c (kcal mol ⁻¹)
5'-CCGATCAC/TC-3' 3'-GC/GTAGTGAG-5'	59.4	0.176	0.179	7.0	6.1
5'-CCGCATCA/CTC-3' 3'-GC/GTAGTGAG-5'	58.3	0.172	0.174	7.0	6.3
5'-CCGCATC/ACTC-3' 3'-GC/GTAGTGAG-5'	44.4	0.136	0.138	3.7	3.2
5'-CCGCAT/CACTC-3' 3'-GC/GTAGTGAG-5'	41.4	0.129	0.130	2.8	2.5
5'-CGCA/TCACTC-3' 3'-GC/GTAGTGAG-5'	33.1	0.104	0.105	2.0	1.8

^aThe top strand of each duplex is represented in the 5' to 3' orientation. The slash indicates the position of the nick in the strand. The corresponding base pairs along the cohesive tracts from top to bottom are 6-bp, 5-bp, 4-bp, 3-bp, and 2-bp, respectively. ^bParameters are in 1 M Na⁺. ^cParameters are at an [Na⁺]_{eff} of 0.217 M.

and is also capable of being distorted by apo-SoxR. The lack of a difference in FRET in the absence and presence of protein indicates that sticky ends containing six nucleotide pairs [6.1 kcal/mol (Table 1)] keep the system too tight to be distorted, implying the transition is complete with less than 6.1 kcal/mol.

It has been estimated by Hidalgo et al.¹¹ that the dissociation constant K_D for the apo-SoxR-soxS promoter complex is 3.8×10^{-10} M. According to the relationship $\Delta G = -RT \ln K_D$, where $R = 1.99 \times 10^{-3}$ kcal mol⁻¹ K⁻¹ and $T = 298$ K, the dissociation free energy for this system is 12.9 kcal mol⁻¹, a value for a system with no sticky ends to disrupt. We estimate that the end point of the binding free energy of apo-SoxR is smaller than this value and is between 3.2 and 6.1 kcal/mol. A more precise end point value could be obtained by modifying the basic sequence to interpolate the values available from the initial sequence, which was done previously.^{16,29} Nevertheless, it is clear from the FRET data that the effect of apo-SoxR on the original TX device (N0) is similar to the effect of shortening the TX device by 2 bp (N-2), and that apo-SoxR binds with a free energy of <6.1 kcal/mol.

In summary, the experiments reported above show that the apo-SoxR protein can bind and distort the TX nanomechanical device, although we cannot tell exactly how this distortion occurs, because of the limitations of the steady-state FRET measurement. With regard to the cohesive tract, we point out that once cohesion is broken by the binding of SoxR, it is no longer in the system, and the system is free to reach the equilibrium conformation associated with binding. It is worth noting that we measure a change in distance corresponding to ~5 Å, and that our experimental error is ~2.5 Å; were we to find a 70° rotation, we would expect a difference of 7 Å, assuming a 2 nm helix axis separation in the TX device. The FRET signal obtained here for the original TX device in the presence of apo-SoxR (N+P) is relatively close to that of the TX device with a 2 bp shortening (N-2) if all the sources of difference are bundled into a rotation; using the same metric, we find that this system is ~1 bp different from the crystal structure of the [2Fe-2S] SoxR-soxS promoter complex. Other MerR family members bend their DNA promoters in the apo form and suppress the transcription.^{30,31} In the holo form, they further unwind the promoters and activate transcription.^{30,31}

Apo-SoxR binds soxS promoter DNA with an affinity equal to that of Fe-SoxR, yet it activates transcription poorly in vitro¹² unless the DNA is negatively supercoiled (H. Ding, E. Hidalgo, and B. Demple, Transcriptional activity of apo-SoxR protein dependent on negative supercoiling of the DNA, manuscript submitted for publication). However, the transcriptional activity of apo-SoxR is smaller than that of oxidized Fe-SoxR, which may be due to the different modes of distortion between the two forms, as well as a smaller degree of distortion by apo-SoxR compared to [2Fe-2S] SoxR.

The DNA nanomechanical device constructed here could be used to investigate the functioning of various DNA regulatory proteins associated with small distortions, by changing the binding site in its top domain. In principle, it could be used to measure even smaller distortions by extending the triple-crossover motif to a quadruple- or quintuple-crossover motif; however, such motifs may be more flexible than the TX motif, leading to other uncertainties. It is also possible to design other sophisticated structured nanomechanical devices responding to different stimuli.²⁹

ASSOCIATED CONTENT

Supporting Information

Titration for the apo-SoxR binding TX nanomechanical device and the sequences of all the molecules used in this study. This material is available free of charge via the Internet at <http://pubs.acs.org>.

AUTHOR INFORMATION

Corresponding Author

*Phone: (212) 998-8395. Fax: (212) 995-4475. E-mail: ned.seeman@nyu.edu.

Present Address

[§]Department of Chemistry, Brown University, 324 Brook St., Providence, RI 02912.

Funding

This research has been supported by Grant CA-37831 from the National Cancer Institute to B.D. and the following grants to N.C.S.: GM-29544 from the National Institute of General Medical Sciences, CTS-0608889 and CCF-0726378 from the National Science Foundation, 48681-EL and W911NF-07-1-0439 from the Army Research Office, N000140910181 from the Office of Naval Research, and a grant from the W. M. Keck Foundation.

Notes

The authors declare no competing financial interest.

ACKNOWLEDGMENTS

We thank Ruojie Sha for valuable discussions about the calculations.

REFERENCES

- Seeman, N. C. (2005) From genes to machines: DNA nanomechanical devices. *Trends Biochem. Sci.* 30, 119–125.
- Yang, X., Vologodskii, A., Liu, B., Kemper, B., and Seeman, N. C. (1998) Torsional control of double stranded DNA branch migration. *Biopolymers* 45, 69–83.
- Mao, C., Sun, W., Shen, Z., and Seeman, N. C. (1999) A DNA nanomechanical device based on the B-Z transition. *Nature* 397, 144–146.
- Yurke, B., Turberfield, A. J., Mills, A. P. Jr., Simmel, F. C., and Newmann, J. L. (2000) A DNA-fuelled molecular machine made of DNA. *Nature* 406, 605–608.

- (5) Yan, H., Zhang, X., Shen, Z., and Seeman, N. C. (2002) A robust DNA mechanical device controlled by hybridization topology. *Nature* 415, 62–65.
- (6) Shen, W. Q., Bruist, M. F., Goodman, S. D., and Seeman, N. C. (2004) A protein-driven DNA device that measures the excess binding energy of proteins that distort DNA. *Angew. Chem., Int. Ed.* 43, 4750–4752.
- (7) Chakraborty, B., Sha, R., and Seeman, N. C. (2008) A DNA-based nanomechanical device with three robust states. *Proc. Natl. Acad. Sci. U.S.A.* 105, 17245–17249.
- (8) Rich, A., Nordheim, A., and Wang, A. H.-J. (1984) The chemistry and biology of left-handed Z-DNA. *Annu. Rev. Biochem.* 53, 791–846.
- (9) LaBean, T., Yan, H., Kopatsch, J., Liu, F., Winfree, E., Reif, J. H., and Seeman, N. C. (2000) The construction, analysis, ligation and self-assembly of DNA triple crossover complexes. *J. Am. Chem. Soc.* 122, 1848–1860.
- (10) Rice, P. A., Yang, S. W., Mizuuchi, K., and Nash, H. A. (1996) Crystal structure of an IHF-DNA complex: A protein-induced DNA U-turn. *Cell* 87, 1295–1306.
- (11) Hidalgo, E., and Demple, B. (1997) Spacing of promoter elements regulates the basal expression of the SoxS gene and converts SoxR from a transcriptional activator into a repressor. *EMBO J.* 16, 1056–1065.
- (12) Hidalgo, E., and Demple, B. (1996) Activation of SoxR-dependent transcription *in vitro* by noncatalytic or NifS-mediated assembly of [2Fe-2S] clusters into apo-SoxR. *J. Biol. Chem.* 271, 7269–7272.
- (13) Ansari, A. Z., Chael, M. L., and Ohalloran, T. V. (1992) Allosteric underwinding of DNA is a critical step in positive control of transcription by Hg-MerR. *Nature* 355, 87–89.
- (14) Demple, B., Ding, Y., and Reiter, T. A. (2007) Harnessing Toxic Reactions to Signal Stress: Reactions of Nitric Oxide with Iron-Sulfur Centers and the Informative Case of SoxR Protein. In *Radicals for Life: The Various Forms of Nitric Oxide* (van Faassen, E., and Vanin, A. F., Eds.) Chapter 7, pp 147–160, Elsevier, Amsterdam.
- (15) Watanabe, S., Kita, A., Kobayashi, K., and Miki, K. (2008) Crystal structure of the [2Fe-2S] oxidative-stress sensor SoxR bound to DNA. *Proc. Natl. Acad. Sci. U.S.A.* 105, 4121–4126.
- (16) Shen, W. Q. (2004) Protein Driven DNA Nanomechanical Devices. Ph.D. Dissertation, New York University, New York.
- (17) Seeman, N. C. (1990) De novo design of sequences for nucleic acid structure engineering. *J. Biomol. Struct. Dyn.* 8, 573–581.
- (18) Seeman, N. C. (1982) Nucleic acid junctions and lattices. *J. Theor. Biol.* 99, 237–247.
- (19) Caruthers, M. H. (1985) Gene synthesis machines: DNA chemistry and its uses. *Science* 230, 281–285.
- (20) Seeman, N. C. (2002) Key experimental approaches in DNA nanotechnology. *Curr. Protoc. Nucl. Acid Chem.*, 12.1.1–12.1.14.
- (21) Demple, B., Ding, H., and Jorgensen, M. (2002) *E. coli* SoxR protein: Sensor/transducer of oxidative stress and nitric oxide. In *Methods in Enzymology* (Packer, L., and Sies, H., Eds.) Protein Sensors of Reactive Oxygen Species: Selenoproteins, Thioredoxin, Thiol Enzymes and Proteins, Vol. 348, pp 355–364.
- (22) Stryer, L. (1978) Fluorescence energy transfer as a spectroscopic ruler. *Annu. Rev. Biochem.* 47, 819–846.
- (23) Jares-Erijman, E., and Jovin, T. M. (1996) Determination of DNA helical handedness by fluorescence resonance energy transfer. *J. Mol. Biol.* 257, 597–617.
- (24) Birac, J. J., Sherman, W. B., Kopatsch, J., Constantinou, P. E., and Seeman, N. C. (2006) Architecture with GIDEON, a program for design in structural DNA nanotechnology. *J. Mol. Graphics Model.* 25, 470–480.
- (25) Förster, T. (1946) Energiewanderung und fluoreszenz. *Naturwissenschaften* 6, 166–175.
- (26) Förster, T. (1948) Zwischenmolekulare energiewanderung und fluoreszenz. *Ann. Phys. (Weinheim, Ger.)* 2, 55–75.
- (27) SantaLucia, J. Jr. (1998) A unified view of polymer, dumbbell, and oligonucleotide DNA nearest-neighbor thermodynamics. *Proc. Natl. Acad. Sci. U.S.A.* 95, 1460–1465.
- (28) SantaLucia, J. Jr., and Hicks, D. (2004) The thermodynamics of DNA structural motifs. *Annu. Rev. Biophys. Biomol. Struct.* 33, 415–440.
- (29) Gu, H., Yang, W., and Seeman, N. C. (2010) DNA scissors device used to measure MutS binding to DNA mispairs. *J. Am. Chem. Soc.* 132, 4352–4357.
- (30) Brown, N. L., Stoyanov, J. V., Kidd, S. P., and Hobman, J. L. (2003) The MerR family of transcriptional regulators. *FEMS Microbiol. Rev.* 27, 145–163.
- (31) Sarkar, S. K., Andoy, N. M., Benítez, J. J., Chen, P. R., Kong, J. S., He, C., and Chen, P. (2007) Engineered Holliday junctions as single-molecule reporters for protein-DNA interactions with application to a MerR-family regulator. *J. Am. Chem. Soc.* 129, 12461–12467.
- (32) Privalle, C. T., Kong, S. E., and Fridovich, I. (1993) Induction of manganese-containing superoxide dismutase in anaerobic *Escherichia coli* by diamide and 1,10-phenanthroline: Sites of transcriptional regulation. *Proc. Natl. Acad. Sci. U.S.A.* 90, 2310–2314.
- (33) Ahsen, N. V., Wittwer, C. T., and Schutz, E. (2001) Oligonucleotide melting temperatures under PCR conditions: Nearest-neighbor corrections for Mg²⁺, deoxynucleotide triphosphate, and dimethyl sulfoxide concentrations with comparison to alternative empirical formulas. *Clin. Chem.* 47, 1956–1961.
- (34) Owczarzy, R., Moreira, B. G., You, Y., Behlke, M. A., and Walder, J. A. (2008) Predicting stability of DNA duplexes in solutions containing magnesium and monovalent cations. *Biochemistry* 47, 5336–5353.
- (35) Geggier, S., and Vologodskii, A. (2010) Sequence dependence of DNA bending rigidity. *Proc. Natl. Acad. Sci. U.S.A.* 107, 15421–15426.